Applied Materials Today 23 (2021) 100994

Contents lists available at ScienceDirect

Applied Materials Today

journal homepage: www.elsevier.com/locate/apmt

Improving capture efficiency of human cancer cell derived exosomes with nanostructured metal organic framework functionalized beads

Sareh Zhand[a], Kun Xiao[b], Sajad Razavi Bazaz[a], Ying Zhu[c], Pritam Bordhan[a,b], Dayong Jin[d,*], Majid Ebrahimi Warkiani[a,d,e,**]

[a] School of Biomedical Engineering, University of Technology Sydney, Sydney, New South Wales 2007, Australia
[b] School of Life Sciences, Faculty of Science, University of Technology Sydney, Sydney, New South Wales 2007, Australia
[c] St George and Sutherland Clinical School, UNSW Sydney, NSW 2052, Australia
[d] Institute for Biomedical Materials and Devices, Faculty of Science, University of Technology Sydney, New South Wales 2007, Australia
[e] Institute of Molecular Medicine, Sechenov First Moscow State University, Moscow 119991, Russia

ARTICLE INFO

Article history:
Received 26 August 2020
Revised 31 January 2021
Accepted 2 March 2021

Keywords:
Exosome
Immunocapture
Flow cytometry
Metal-organic framework
ZIF-8

ABSTRACT

Extracellular vesicles (EVs) have emerged as an invaluable tool for analyzing the physiological processes and an alternative source of disease diagnostic and prognostic biomarkers in liquid biopsies. Exosomes are a subset of EVs offer a window into altered cellular or tissue states, and their detection potentially offers a multicomponent early-stage diagnostic readout. Immunocapture and flow cytometry analysis of exosomes using micron-sized beads has been reported to be a reproducible technique for analysis of exosome surface markers. Nevertheless, the capture capacity remains poor due to limited available surface area. In this study, we have proposed a nanocoating strategy using metal-organic framework (MOF) materials, in particular, Zeolitic Imidazolate Framework-8 (ZIF-8), for highly efficient capturing of low concentration of exosomes from minimally processed samples. In this method, a ZIF-8 thin film was formed on polydopamine-polyethyleneimine (PDA-PEI) coated polystyrene microbeads to improve antibody immobilization due to the larger surface area provided by the MOF microstructures. This novel coating enabled us to detect as little as 50 exosomes per 10 μm polystyrene bead functionalized with ZIF-8/PDA-PEI, which is 180 times higher than the previously reported methods using naked microbeads. This coating requires a lower concentration of antibody to capture exosomes on the surface of microbeads compared to the standard protocols. More importantly, the higher concentration of exosomes on each bead surface provides the opportunity (i.e., higher signal intensity) to sort the beads using fluorescence-activated cell sorting, facilitating molecular analysis of post fractionation exosomes. Additionally, the exosomes can easily be detached from the coated microbeads using EDTA, limiting the usage of harsh chemicals. The procedure described here can be easily reproduced and employed regardless of the biological sample used to obtain exosomes.

© 2021 Elsevier Ltd. All rights reserved.

1. Introduction

Cancer is one of the leading causes of mortality around the world and is considered to be a global health issue [1]. This necessitates early-stage detection of cancers with a non-invasive and targeted therapeutic approach to improve patient's quality of life and chances of survival [2]. This coincides with the need to prioritize ongoing scientific research towards the discovery of reliable cancer indicators/biomarkers and optimize their isolation and characterization processes facilitating the development of more reliable cancer diagnostic platforms [3].

It has been shown that at the early stage of cancer, some unique compounds that are favorable for early detection of cancer, including circulating tumor cells (CTCs), extracellular vesicles (EVs), and circulating tumor DNA (ctDNA), are released [4-6]. Thus, platforms for measuring the number of CTCs, protein expression profiling of EVs, or analyzing the mutations of ctDNA existing in the biological samples of cancerous patients enables monitoring of the dynamic cancer development and evaluation of the therapeutic outcome. These so-called liquid biopsy methods play a pivotal role in the early-stage cancer detection [4,7-10].

* Corresponding author.
** Corresponding author at: School of Biomedical Engineering, University of Technology Sydney, Sydney, New South Wales 2007, Australia.
E-mail addresses: Dayong.Jin@uts.edu.au (D. Jin), majid.warkiani@uts.edu.au (M.E. Warkiani).

https://doi.org/10.1016/j.apmt.2021.100994
2352-9407/© 2021 Elsevier Ltd. All rights reserved.

Among these three classifications of biomarkers, EVs are a promising category. EVs are lipid bilayer-encapsulated particles released from most mammalian cells. Exosomes are a type of EVs formed by inward budding of late endosomes and have a diameter of 30–150 nm [11]. They carry some biomolecules such as proteins, DNA species (mitochondrial DNA and nuclear DNA), RNA species (mRNA, microRNA, and lncRNA), lipids, and metabolites that contain the information of the tissue that they originated from [12]. Emerging evidence has shown that these sources of biomarkers could be beneficial for the early diagnosis as well as prognosis of cancers and monitoring the tumor condition [4,13,14]. Exosomes notably play an essential role in physiological and pathological processes, including immune response [15], signal transduction [16], tumor initiation, progression, invasion, and metastasis [17,18]. Despite the broad diversity in origin of exosomes, they are all composed of some common structural and functional proteins, such as Rab GTPase, *N*-ethylmaleimide-sensitive factor attachment protein receptors (SNAREs), annexins, Alix, Tsg101, and tetraspanins family (CD9, CD81, CD82, and CD63) [19]. With the advancement of biomedical technology, exosomes as a new type of biomaterials have attained important research value; therefore, the isolation of exosomes from a wide range of cell fragments is imperative [20]. However, despite gaining more attraction for investigating the composition and function of exosomes, there is still a lack of standardized methods for the isolation and purification of exosomes [21].

Some techniques that are employed for the enrichment of exosomes prior to characterization include ultracentrifugation based separation [22], polymer-based precipitation [23], density gradient separation, ultrafiltration, size exclusion chromatography, and microfluidics [24,25]. Each of these techniques has their advantages and disadvantages in the context of exosome purity and sample recovery based on potential downstream usage. Among these, ultracentrifugation is one of the most common exosome separation techniques that relies on the sequential separation of particles by sedimentation dependent on their size and density using a series of centrifugal forces and duration [26]. While a number of scientific developments continue to be explored towards the enhancement of exosome isolation, currently ultracentrifugation, even with its numerous drawbacks, remains to be the gold standard technique [27].

Another approach to isolate and purify exosomes is the immunoaffinity-based method, which relies on the separation of specific exosomes based on the expression of surface proteins, including the common exosome surface markers (CD9, CD63, and CD81) as well as disease-specific markers (chondroitin sulfate peptidoglycan 4, epithelial cellular adhesion molecule (EpCAM)), or heat shock protein and heparin [28]. This method is usually used as an additional step combined with ultracentrifuge to increase the purity of isolated exosomes. Following the immune-affinity capture, the flow cytometry is regarded as an advantageous tool for the analysis and characterization of cell-derived particles including exosomes that attached to microbeads, owing to its robust statistical power and its multi-parametric capabilities [29–32]. It has been used effectively to characterize exosomes from multiple types of cells, including Mel526 melanoma cell lines [33], K562 human erythromyeloblastoid leukemia cells [34], and PC3 prostate cancer cells [21]. Another approach is a method of using microfluidic devices to isolate exosomes based on several principles including immunoaffinity, size, and density [35]. The immunomicrofluidic technique has also been successfully employed as well as bead-based microarray platforms to isolate and characterize exosomes derived from multiple human cancer cell lines and patient's plasma samples [36-38]. So far, multiple microstructures were configured to improve exosome capture efficiency; Nevertheless, capture capacity in bead-based flow cytometry remains limited due to the insufficient surface area on the beads and antibody immobilization density.

Recently, metal-organic frameworks (MOFs) materials have been proposed as a potent nanocoating strategy for improving the sensitivity and selectivity in cancer biomarkers detection [39]. The MOFs structure consists of metal ions and organic linkers, making the crystalline structure uniform with tunable porosity. By increasing the surface to volume ratio, this structure provides more surface area for analytes reaction as well as capturing of biomarkers with various structures and reactivity. The efficient immobilization of antibodies on the nanoscale surface enhances the capturing capacity of the target. Moreover, the MOFs also provide room for capturing analytes inside the framework within their dynamic geometrical shapes. Their versatile molecular composition offers selective targeting of biomarkers [39]. Owing to the flexible functionalization of MOFs, tunable pore sizes, high loading efficiency and biodegradability, they can be considered as potential platforms enabling the early detection of cancer [39]. Among the MOFs, Zeolitic Imidazolate Framework-8 (ZIF-8) shows excellent ability for immobilization of bio-macromolecules, including proteins, enzymes, and DNA [40,41]. Moreover, its facile degradation under mild conditions allows easy detachment of immobilized molecules [42]. These features make ZIF-8 a suitable candidate for antibody immobilization.

In this study, for the first time we have introduced the application of MOF to improve the capture efficiency of exosomes by flow cytometry. We have described the optimized ultracentrifugation and immuno-affinity bead-based capture process followed by flow cytometry analysis for exosome detection and characterization based on the presence of CD63, CD81, CD9 proteins as well as EpCAM and programmed death-ligand 1(PD-L1) biomarkers. By examining all three exosome biomarkers the potential heterogeneity issue in different patient samples (i.e. some samples show just one marker instead of the other two) would be excluded [43]. This new antibody immobilization method involves coating the surface of polystyrene beads with the ZIF-8 as a representative of MOF to form a stable complex on a polydopamine-polyethyleneimine (PDA-PEI) pattern. The MOF-based antibody immobilization improved the efficiency of the exosome capturing, demonstrating its potential to significantly improve current detection methods. This study aimed to improve the limit of detection (LOD) for exosome capturing and increasing the sensitivity and specificity of immunocapture using beads@ZIF-8/PDA-PEI, thereby allowing FACS/flow cytometry-based sorting of exosome attached beads (higher signal intensity), for post fractionation molecular analysis, while consuming minimal amounts of antibody.

2. Materials and methods

2.1. Reagents

10 μm polystyrene beads with a concentration of 1.87×10^8 particles/mL were purchased from Bangs Laboratories Inc (USA). Primary antibodies including purified anti-human CD63 (Clone H5C6), purified anti-human CD9 (Clone HI9a), purified anti-human CD81 (Clone 5A6), anti-human EpCAM (Clone CO17-1A), and anti-human PD-L1(Clone MIH3), secondary antibody HRP Goat anti-mouse IgG (405306) and detector antibodies for flow cytometry: anti-CD63 APC (353008), anti-CD9-FITC (312104), anti-CD81-PE (349506), anti-PD-L1-PEcy7(374506), anti-EpCAM-PE/Dazzle™ 594 (369818) were obtained from Biolegend (USA). BenchMark™ Pre-stained Protein Ladder (10748010), Novex™ Sharp Pre-stained Protein Standard (LC5800), RIPA Lysis and Extraction Buffer (89900, Thermo Fisher, USA), Pierce BCA protein assay kit (Pierce Biotechnology), 4X Bolt™ LDS Sample Buffer (B0007, Thermo Fisher), polyvinylidene difluoride (PVDF) membranes (Thermo Fisher, USA), Bolt™ 4–12% Bis-Tris Plus Gels, (NW04120BOX, In-

vitrogen, USA) and SuperSignal™ West Dura Extended Duration Substrate (37071, Thermofisher, USA) were purchased. Phosphate buffered saline (PBS), 2-methylimidazole, Dopamine hydrochloride , Polyethyleneimine (PEI, Mw=1000 Da), Tris (hydroxylmethyl) aminomethane, Bovine serum albumins (BSA), hexamethyldisilazane (HDMS), MES (M3671), N-(3-dimethylaminopropyl)-N′-ethylcarbodiimide hydrochloride (EDC, E7750), and zinc nitrate hexahydrate were purchased from Sigma–Aldrich (USA).

2.2. Cell culture and preparation of conditioned medium (CM)

Three different cancer cell lines (i.e., MDA-MB-231 and MCF-7 breast cancer cells, HeLa cervical cancer cell) were cultured in Dulbecco's modified Eagle's medium (DMEM, Gibco, UK) supplemented with 10% (v/v) fetal bovine serum (FBS, Gibco, UK), 100 U/mL penicillin and

100 mg/mL streptomycin (Gibco, UK) in a T175 tissue culture flask (ThermoFisher, USA) and incubated at 37 °C in a 5% CO_2 humidified incubator. Once cells reached 70% confluency, (approximately 3×10^7 cells), the supernatant was carefully discarded, and the cells were washed twice with phosphate buffer saline (PBS). Then, the cells were cultured in an exosome-free medium (DMEM without FBS) under hypoxic conditions for 48 h at 37 °C in a 5% CO_2 humidified incubator, and the culture medium was collected for further experiments.

2.3. Isolation of extracellular vesicles by ultracentrifugation

Media containing released EVs was collected and subjected to multiple centrifugation steps including 300 × g for 10 min and 2000 × g for 10 min followed by 10,000 × g (R18A rotor, HITACHI CR22N, Japan) (for 30 min to remove cells, dead cells and cell debris, then filtrated through sterile 0.22 μm syringe filter (Merck Millipore, USA). The conditioned media underwent ultracentrifugation at 100,000 × g for 120 min (F37L carbon fiber rotor, Sorvall WX ultra series, ThermoFisher, USA). The supernatant was removed, and pellets that contained EVs and contaminating proteins were re-suspended in a separate ultracentrifuge tube in PBS, previously filtered through 0.22 μm syringe filter, and centrifuged a second time at 100,000 × *g* for 120 min. The supernatant was removed, and the exosome pellet was re-suspended in ~100 μL filtrated PBS. The exosomes were stored at −80 °C until use. All centrifugation steps were performed at 4 °C.

2.4. Nanoparticle tracking analysis

Nanoparticle tracking analysis (NTA) was performed on a NanoSight LM14 system (NanoSight Technology, Malvern, U.K.) equipped with a 532 nm green laser for determining the exosome concentration and size distribution. 100μL isolated exosome samples were diluted to 500μL with freshly filtered PBS (0.22 μm filter) and loaded into the detection chamber by syringe. The camera was manually set and kept the same for all samples with a slider shutter 650 and slider gain 50. 30 s videos were recorded, and the number of captures was 5. The detection threshold was set to 6, and blur and max jump distance were automatically set. The temperature was maintained at 25 °C. The data were processed by the NTA software (NTA version 3.3; Malvern Instruments, Malvern, U.K).

2.5. Western Blot

In order to evaluate the purity of the exosome preparations and to demonstrate the absence of cellular contaminants from cell lysate in our exosome preparation, the isolated exosomes and the corresponding cells were lysed by adding an equal volume of RIPA Lysis and Extraction Buffer (89900, Thermo Fisher, USA). The protein concentration of the exosomes and cell lysates were measured using a Pierce BCA protein assay kit (Pierce Biotechnology), according to the manufacturer's instructions. For Western Blot analysis, exosome proteins (2×10^8 particles; ~5 μg) and cell lysate (5 μg) were resolved using Bolt™ 4–12% Bis-Tris Plus Gels (NW04120BOX, Invitrogen, USA). Samples were diluted in 4X Bolt™ LDS Sample Buffer (B0007, Thermo Fisher) and heated up at 70 °C for 10 min, then transferred on to polyvinylidene difluoride (PVDF) membranes (Thermo Fisher, USA). The PVDF membrane was blocked for 30 min at room temperature with 5% non-fat powdered milk in PBS-T (PBS and 0.5% Tween-20) and incubated overnight at 4 °C with the following primary antibodies separately: anti-human CD63 (353039 Biolegend, USA), anti-human CD9 (312102 Biolegend, USA), and purified anti-human CD81 (349502, Biolegend, USA) (1:500 in PBS-T). In the next step, the blots were incubated with appropriate HRP-conjugated Goat anti-mouse IgG secondary antibody (1:2000) in PBS-T for 1 h at 37 °C. The blots were washed three times with PBS-T buffer for 10 min after each incubation step then visualized using with a SuperSignal™ West Dura Extended Duration Substrate (37071, Thermofisher, USA). The mentioned proteins were resolved under non-reducing conditions.

2.6. Transmission electron microscopy (TEM)

To investigate the morphology of the exosomes isolated by ultracentrifugation, transmission electron microscopy (TEM) was used. Briefly, 5 μl of exosome sample was fixed with 2.5% formaldehyde and applied to 300-square mesh copper grids coated with a thin formvar carbon film. The grids were subsequently negatively stained with 1% UAR-EMS Uranyl acetate replacement stain and incubated for 30 min. Grids were washed with PBS and dried with filter paper. The exosome sample was observed using a TEM Tecnai T20 microscope operating at 180 kV and equipped with Gatan 894 2k x 2k camera to get high-quality digital images.

2.7. PDA-PEI coating of 10 μm polystyrene beads

10 μm polystyrene beads were coated with a thin layer of PDA-PEI based on a previously published protocol [44]. A PDA film can form on organic/inorganic surfaces through self-polymerization of dopamine under alkaline conditions [45]. PEI in the dual polymerization of PDA-PEI, endures Michael addition or Schiff-base reactions with a catechol group in PDA to produce a strong bioadhesive layer on the surface of the substrate. Therefore, the role of PEI was as a crosslinking agent with PDA [46]. Briefly, 1 mL of polystyrene beads (1.87×10^8 beads) was treated with 5 mL of freshly prepared solution of dopamine hydrochloride (2 mg/mL), PEI (1000 MW, 2 mg/mL) in Tris-buffer solution (0.05 M, pH 8.5), then sonicated for 5 min and left in solution with mild stirring overnight at room temperature. The beads were washed three times with Milli-Q® water through the centrifugation steps at 3000 × *g* for 5 min. For each experiment, a fresh dopamine hydrochloride solution was used to prevent premature polymerization of dopamine.

2.8. ZIF-8@PDA-PEI coating of 10 μm polystyrene beads

In this study, ZIF-8 was used as a representative MOF structure. ZIF-8 was synthesized through a self-assembly process, as previously described [44]. Briefly, the ZIF-8 precursor solution was prepared from zinc nitrate hexahydrate, $Zn(NO_3)_2 \bullet 6H_2O$, (0.027 g) and 2-methyl imidazole, (0.566 g) in 10 mL Milli-Q® water. The ZIF-8 solution was gently added to beads@PDA-PEI and incubated for 2 h

at room temperature without agitation. The resultant beads@ZIF-8/PDA-PEI were washed three times with PBS following the centrifugation at 3000 × g for 5 min and used for highly efficient capturing of exosome biomarkers.

2.9. Surface characterization

The structure of the beads@ZIF-8/PDA-PEI and beads@PDA-PEI was characterized using microscopy imaging techniques. Scanning electron microscopy (SEM, ZEISS SUPRA55VP, USA) was used to probe the surface morphology of the modified polystyrene beads. In order to achieve a good conductivity, the modified surface of polystyrene beads was sputter-coated with a 20 nm Au/Pd coating under vacuum. SEM images were taken with an accelerating voltage of 15 kV. The chemical composition of the modified polystyrene beads@PDA-PEI and polystyrene beads@ZIF-8/PDA-PEI was analyzed by Fourier-transform infrared spectroscopy (FT-IR) (MIRacle 10, Shimadzu, USA). FT-IR spectra were acquired in the range of 4000–400 cm^{-1} with a resolution of 4 cm^{-1} and averaging 16 scans for each spectrum for three times. Furthermore, powder X-ray diffraction (XRD) (D8 Discover BRUKER) was performed to identify the ZIF-8 crystalline structure on the surface of the PDA-PEI-coated polystyrene beads. Crystallographic data of the antibody@ZIF-8/PDA-PEI patterns was obtained by scanning the sample through a 2θ range of 5–40° with a step size of 0.019° and 1 s per step. The XRD data analysis was performed using High Score Plus software and compared with the database from the International Center for Diffraction Data.

2.10. Preliminary titrations of capture antibodies on polystyrene beads and beads@ZIF-8@PDA-PEI

Titrations were set up in two separate set of microtubes; the first set included 1 mg (1.87×10^6) carboxylate polystyrene beads in each microtube and the other set with constant amount of beads@ZIF-8/PDA-PEI. Each set of above mentioned microtubes were co-incubated with 1.5, 0.75, 0.35 µg of anti-CD63-APC (353008), anti-CD9-FITC (312104), anti-CD81-PE (349506), anti-PD-L1 -PEcy7 (374506), and anti- EpCAM-PE/Dazzle™ 594 (369818) antibodies separately at 37 °C for 90 min to find out the best fluorescent signal intensity of immobilized antibody as well as the optimal concentration of antibodies for saturating the whole surface of microbeads and prevent the nonspecific antibody binding. After incubation, the beads were washed 3 times with PBS containing 0.05% Tween 20 through the centrifugation step. Finally, 1 ml of PBS was added to each sample and subjected to flow cytometry analysis (CytoFLEX LX, Beckman Coulter, USA). A histogram overlay was drawn using FlowJo V10 software for all mentioned antibodies in the polystyrene beads versus polystyrene beads@ZIF-8/PDA-PEI. After the determination of optimal capture conditions for antibodies, they were routinely implemented in following experiments.

2.11. Comparison between the efficiency of ZIF-8/PDA-PEI and EDC in antibody immobilization

In brief, covalent coupling was done using EDC (2.5 mg/mL) that incubated with 1 mg of polystyrene beads in MES buffer (pH 5.7) at 37 °C for 30 min. After incubation, beads were washed with PBS using the centrifugation step and the supernatant was discarded. Next, quenching solution with primary amine source and 0.05-1% (w/v) blocking molecule was added and mixed gently for 30 min. Following the washing step, the 1.5 µg of fluorescent antibodies including anti-CD63-APC (353008), anti-CD9-FITC (312104), anti-CD81-PE (349506), anti-PD-L1-PEcy7 (374506), anti-EpCAM-PE/Dazzle™ 594 (369818) were co-incubated with 1 mg of polystyrene beads for 90 min at 37 °C. Then, the beads were washed 3 times with PBS containing 0.05% Tween 20 using the centrifugation step and 1 mL of PBS added to each sample for flow cytometry analysis. The Mean Fluorescent Intensity (MFI) was detected using FlowJo V10 software and the histogram overlay was drawn for all mentioned antibodies in the polystyrene beads versus polystyrene beads@ZIF-8/PDA-PEI and the polystyrene beads functionalized with EDC.

2.12. Evaluation of antibody immobilization using protein binding measurement

To evaluate the sensitivity of the MOF for antibody immobilization on polystyrene beads, three platforms were tested including carboxylate polystyrene beads , carboxylate polystyrene beads coated with EDC and polystyrene beads@ZIF-8/PDA-PEI. They were all co-incubated with a constant concentration of the anti-CD63, anti-CD81, anti-CD9, anti-EpCAM and anti-PD-L1 antibodies (1.5 µg per 1.87×10^6 particles) for 90 min at 37 °C. After incubation, the beads were centrifuged for 5 min at 3000 × g and the supernatant were collected to measure the protein concentration. A Pierce BCA protein assay kit (Pierce Biotechnology) was used to measure the protein concentration of unbound antibodies in the sample.

2.13. Determination of exosome capture efficiency in polystyrene beads and beads@ZIF-8/PDA-PEI

For quantitative detection of exosome-associated surface proteins, an on-bead direct immunoassay was employed, as illustrated in Fig. 1. The exosomes were captured on the polystyrene beads and on the bead@ZIF-8/PDA-PEI that was previously functionalized with anti-CD63, anti-CD81, anti-CD9, anti- EpCAM and anti-PD-L1. The concentration of antibodies and the number of beads was kept constant in all steps [1.5 µg antibody per 1 mg (1.87×10^6) beads].

To test the sensitivity of the MOF for exosomes capture efficiency, the serial dilution of exosomes isolated from each mentioned cell line was used in two separate set of microtubes- one containing beads and the other set contain beads@ZIF-8/PDA-PEI. In this sense 200, 100, 50, and 25 exosomes per bead and for 50,000 beads equal to 1×10^7, 5×10^6, 2.5×10^6, and 1.25×10^6 particles (corresponding to 250 ng, 125 ng, 62.5 ng and 31.2 ng) were co-incubated with above mentioned beads for 18 h at 4 °C without agitation and in a control group BSA was used instead of exosomes. After incubation, the tubes were subjected to centrifugation at 3000 × *g* for 5 min to remove excess reacted exosomes by washing twice with PBS/0.05% Tween 20. The complexes containing bead/antibody/exosome were then co-incubated with the labeled detection antibodies, including anti-CD63-APC (353008), anti-CD9-FITC (312104), anti-CD81-PE (349506), anti-PD-L1-PEcy7 (374506), anti-EpCAM-PE/Dazzle™ 594 (369818) for 90 min at 37 °C. Next, the complexes were washed 3 times with PBS using centrifugation at 3000 × g for 5 min and were re-suspended in 1 mL of PBS for flow cytometry analysis. Samples were run for approximately one minute and 10,000 events were acquired. Gates were set on the bead fraction visible in the FSC/SSC light scatter. The percentage of positive beads was measured, and the histogram overlay was drawn for all the polystyrene beads versus polystyrene beads@ZIF-8/PDA-PEI using FlowJo V10 software. To better visualize the beads with attached exosomes , one droplet of beads/exosome complex was mounted on fluorescent microcopy slides. For fluorescent imaging, the MCHE and FITC channels were used (OLYMPUS IX73, Japan), and to set the treshold line, the polystyrene beads containing BSA instead of exosomes and with detector antibodies were used as a control. Images were analyzed with the ImageJ software.

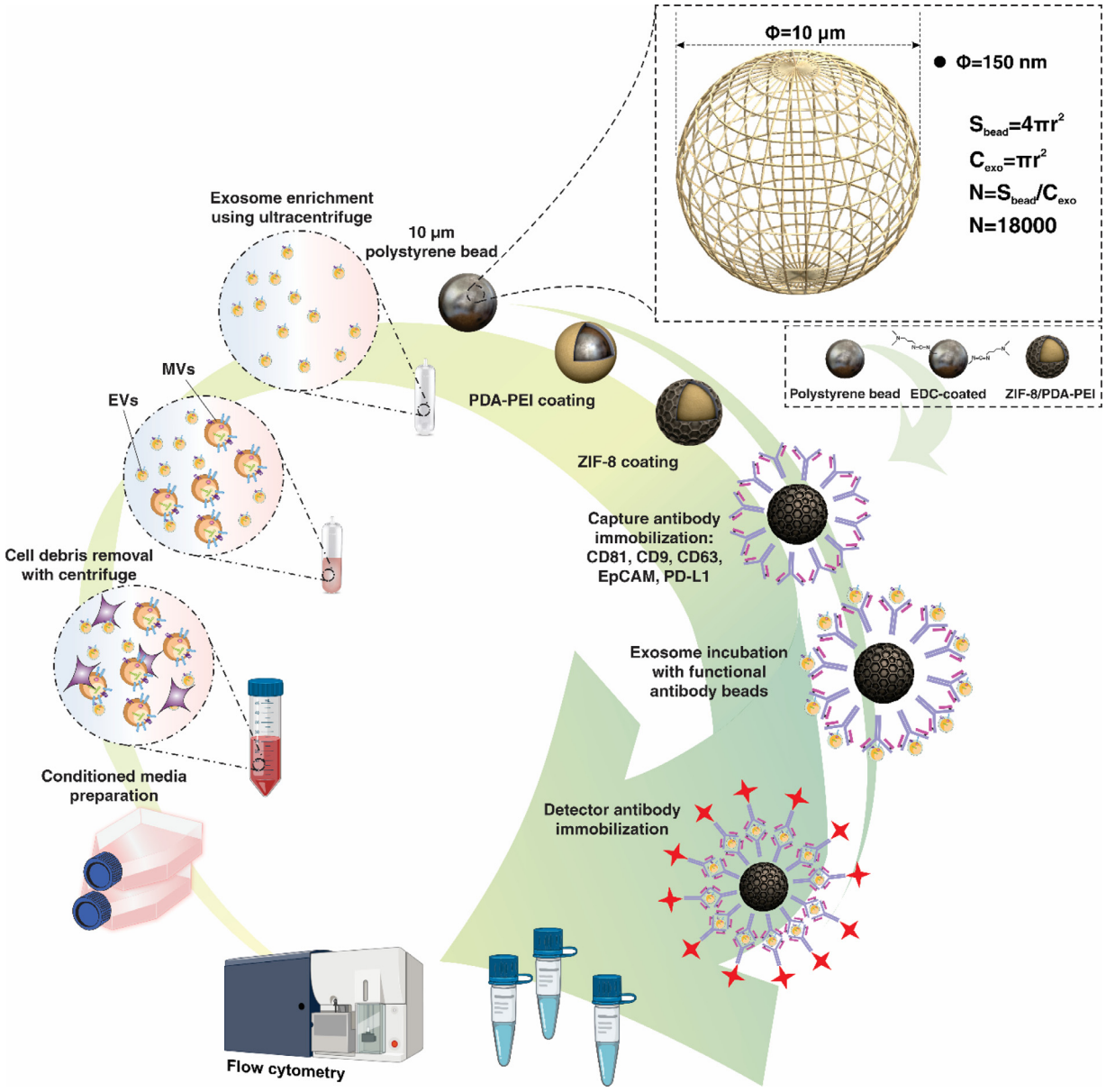

Fig. 1. The workflow of detecting pre-enriched exosomes using surface modification of polystyrene beads with ZIF-8/ PDA-PEI platform following the flowcytometry. The 10 μm polystyrene beads coated with thin layer of ZIF-8/PDA-PEI (beads@ZIF-8/PDA-PEI) incubated with the 1.5 μg of capture anti-CD9, anti-CD63, anti-CD81 as well as anti-EpCAM and anti - PD-L1 antibodies. Following the addition of certain concentrations of pre-enriched exosomes and incubation for 18 h at 4°C, the detector antibodies of anti-CD63-APC, anti-CD9-FITC, anti-CD81-PE, anti-PD-L1 PEcy7, anti-EpCAM-PE/Dazzle™ 594 were added to the mentioned platform and subjected to flowcytometry. The efficacy of antibody immobilization was evaluated in carboxylate polystyrene beads, the carboxyl polystyrene beads functionalized with EDC and the beads@ZIF-8/PDA-PEI platform.

2.14. SEM images of polystyrene beads with exosomes

The isolated exosomes were immobilized on 10 μm polystyrene beads that were previously functionalized with one of these specific capture antibodies (i.e., anti-CD81, anti-CD9 or anti-CD63) through immunoassay process and one droplet of the mixture was mounted on coverslip fixed with 2.5% glutaraldehyde and 2% paraformaldehyde in 100 mM PBS for 30 min. The dehydration process was performed using 50%, 60%, 70%, 80%, 90% and 100% ethanol for 20 min following the addition of hexamethyldisilazane (HDMS, Sigam, USA) in ratio of 1:2 with 100% ethanol into fixed samples for 20 min. Next, a ratio of 2:1 HDMS with 100% ethanol was added to samples and incubated for another 20 min. Finally, the samples were incubated with 100% HDMS for 20 min and dried overnight. The fixed samples were sputter-coated with a 20 nm Au/Pd coating under vacuum. SEM images were taken with an accelerating voltage of 15 kV.

3. Results

3.1. Surface characterization

The structure of the polystyrene beads@ZIF-8/PDA-PEI was characterized using microscopy imaging and spectroscopic techniques. SEM images showed the distinct morphologies of polystyrene beads with and without the ZIF-8 precursors (Fig. 2A, 2B) as well as the polyhedral morphology of pristine ZIF-8 in beads@ZIF-8/PDA-PEI platform. Self-polymerization of dopamine under alkaline conditions contributes to forming a PDA film on organic/inorganic surfaces [45], and PEI was used as a crosslink-

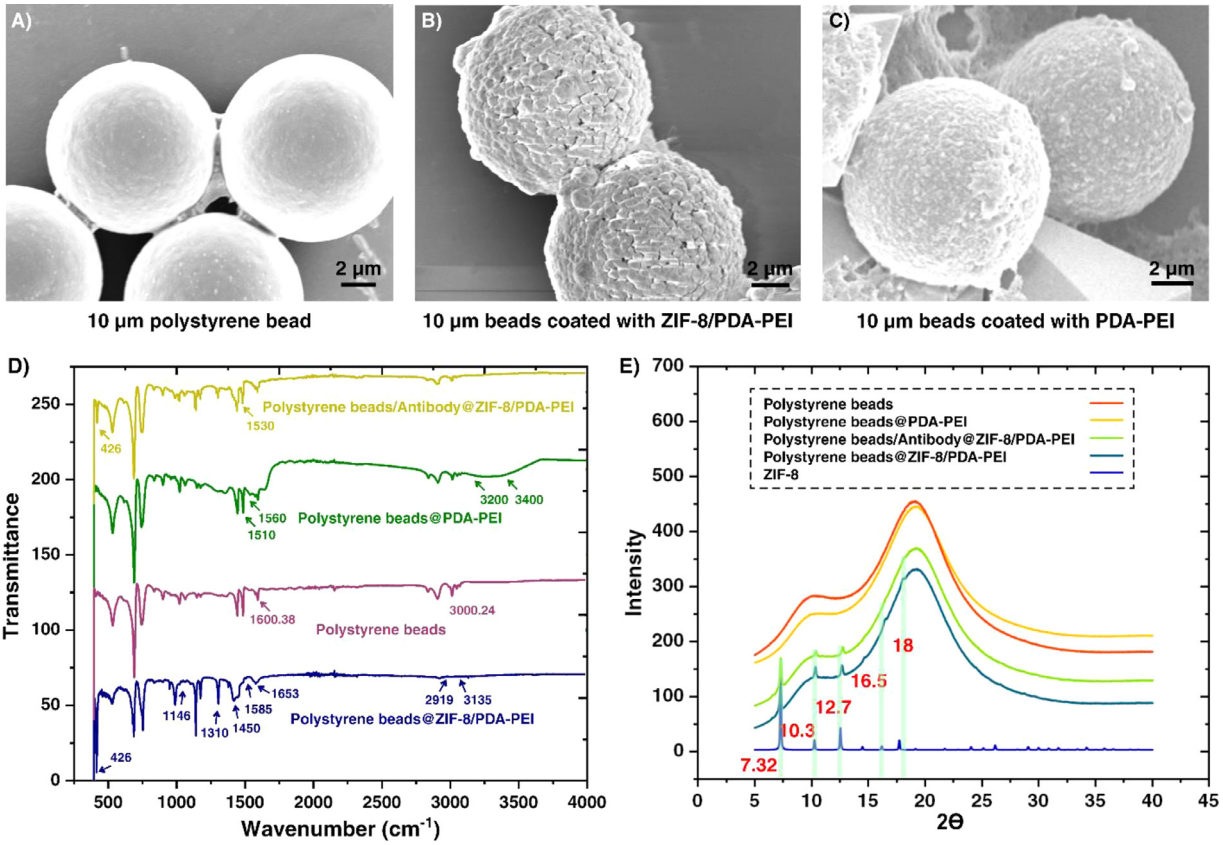

Fig. 2. SEM images of (A) 10 µm polystyrene bead, (B) beads@ZIF-8/PDA-PEI, (C) beads@PDA-PEI at 5000x magnification (Scale bar: 2 µm). (D) FT-IR spectra of polystyrene beads@ZIF-8/PDA-PEI with antibody, polystyrene beads@ZIF-8/PDA-PEI, PDA-PEI coated polystyrene beads and polystyrene beads. Measurements were done from 4000 to 400 cm^{-1} and PDA-PEI showed intensive peak at 1650cm^{-1} whilst ZIF-8 showed important peak at 426cm^{-1}. (E) XRD patterns of polystyrene beads@ZIF-8/PDA-PEI with antibody, polystyrene beads@ZIF-8/PDA-PEI, PDA-PEI coated polystyrene beads and polystyrene beads. The intensive peaks at 7.3, 10.3, 12.7, 16.5, and 18, which are specific for ZIF-8 crystalline structure prove the dense formation of ZIF-8 crystalline layer on the surface of polystyrene beads.

ing agent of PDA [46]. The SEM image showed that the PDA-PEI coating formed a thin, uniform, and dense film on top of the polystyrene beads (Fig. 2C). The SEM images indicated that the polystyrene beads were successfully coated with a PDA-PEI and ZIF-8 layer. The conditions used to achieve a dense coating of PDA-PEI and ZIF-8 on the surface of polystyrene beads were obtained from our previous study [47]. The FT-IR provides useful information about the functional groups present in the structures of PDA-PEI and ZIF-8 (Fig. 2D). Sharp peak detected at 426 cm^{-1} was attributed to Zn–N stretching vibration band, which confirmed the formation of an imidazolate through the chemical combination of zinc ions and nitrogen atoms of the methyl imidazole groups [48]. The FT-IR spectrum of the polystyrene beads coated with PDA-PEI showed a sharp peak in the 1510–1560 cm^{-1} range, which was attributed to N–H vibrations. The FT-IR spectrum with stretches at 1530 cm^{-1} in the polystyrene beads@ZIF-8/PDA-PEI with antibody confirms the presence of antibodies that corresponded with the characteristic amide II band (mainly from a combination of NH bending and CN stretching modes). Moreover, strong interactions between the antibody and the ZIF-8, due to the coordination between the Zn cations and the carbonyl group of the protein, could be concluded by shifting the amide vibrational mode for the antibodies to a higher wave number. The FT-IR results for ZIF-8 and polystyrene beads@ZIF-8/PDA-PEI were consistent with the results of our previous study on coating the ELISA wells with ZIF-8/PDA-PEI [47].

The XRD pattern of polystyrene beads@ZIF-8/PDA-PEI consisted of a broad peak owing to the presence of amorphous PDA-PEI and sharp peaks displayed by simulated ZIF-8 patterns [49]. Additionally, for polystyrene beads@ZIF-8/PDA-PEI with antibody, the discrete peaks recognized were at 2θ of 18.02°, 12.7°, 10.3°, and 7.3°, corresponding to 222, 211, 200, and 110, orientations, respectively (Fig. 2E). These results prove the existence of the crystal structure of ZIF-8.

3.2. Exosome characterization

There are two important components for exosome characterization, which include particle size and concentration. To this end, exosomes were characterized by NTA and complemented with Western Blot and TEM (Fig. 3A-C). The size distribution of exosomes using NTA showed a sharp peak at 144, 163, and 173 nm, and majority of the exosomes had a mean size of 130.2 +/- 1.9 nm (Mean +/-Standard Error; Standard Deviation: 82.8 nm). The concentration of 5.85 × 10^8 +/- 1.21 × 10^7, 5.42 × 10^8 +/- 4.02 × 10^7, and 1.8 × 10^8 +/- 2.34 × 10^7 particles/mL was determined for MDA-MB231, MCF-7, and HeLa cell lines derived exosomes, respectively (Fig. 3A-C). The presence of common exosome markers such as CD63, CD81, and CD9 in extracted exosomes from MDA-MB231, MCF-7 and HeLa cell lines as well as the correspondent cell lysate was detected using the Western Blot (Fig. 3D). The TEM image of enriched exosomes showed that the expected size range and morphology of them are consistent with NTA results (Fig. 3E I) and they are round shape without aggregation. The SEM images of 10 µm polystyrene beads in comparison to the ones covered with exosomes confirmed the size distribution of exosome and demonstrated the characteristic round-cup morphology (Fig. 3EII, III). The SEM images of beads@ZIF-8/PDA-PEI covered with exo-

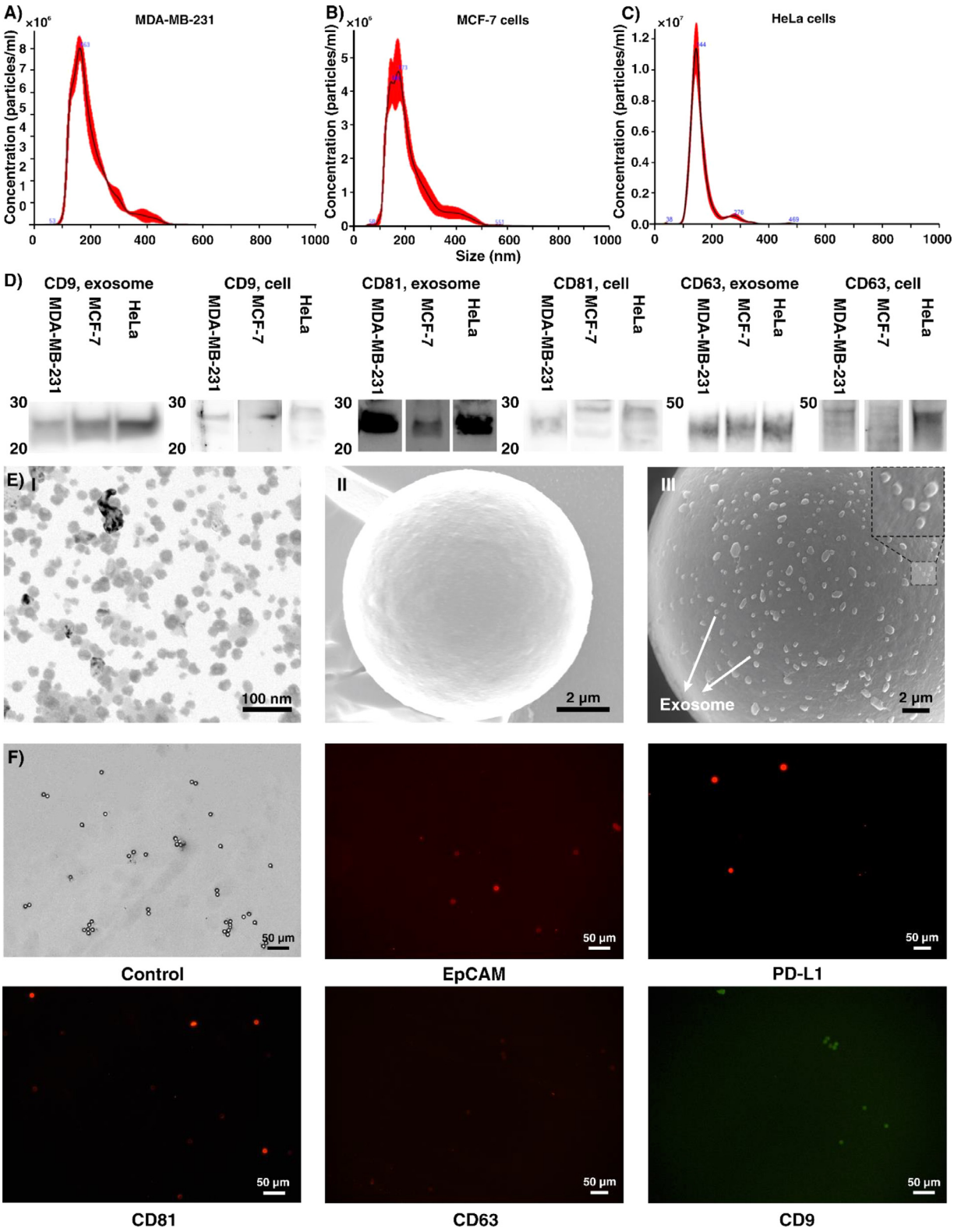

Fig. 3. Characterization of cancer cell-derived exosomes. (A) Nanoparticle tracking analysis (NTA), of exosomes isolated from MDA-MB231, (B) MCF-7 and (C) HeLa cell culture supernatant. For NTA, average size and concentration were obtained in a Nanosight equipment capturing 30 s videos and the number of captures were 5 and camera level was set manually. (D) Western Blot analysis of exosomes and cell lysates from MDA-MB231, MCF-7 and HeLa cell lines. The exosomes as well as the cell lysates were loaded on SDS-PAGE and immunoblotted for antibodies against tetraspanins [anti-CD9, -CD63 and -CD81]. A gel was run under non-reducing conditions with 5 µg cell lysate and 2 × 10^8 exosome particles; ~5 µg, for CD9, CD63 and CD81 detection. The exposure time was 35 s. (E) Microscopic image of exosomes (I)TEM images of isolated exosomes from cell culture supernatant (Scale bar: 100 nm). SEM images of (II) 10 µm polystyrene bead, (III) 10 µm polystyrene bead covered with exosome at 13000x magnification (Scale bar: 2 µm). (F) Fluorescent image of 10 µm polystyrene beads coated with CD9, CD81, CD63, EpCAM and PD-L1 positive exosomes. The polystyrene beads were functionalized with anti-CD9, anti-CD81, anti-CD63, anti-EpCAM and anti-PD-L1 antibodies as capture antibodies respectively, and anti-CD9-FITC, anti-CD81-PE, anti-CD63-APC, anti-EpCAM-PE/Dazzle™ 594 and anti-PD-L1-PE Cy7 antibodies were used as detector.In this experiment; 800 exosomes per 10 µm polystyrene beads were used for capturing CD81, PD-L1, EpCAM positive exosomes using fluorescent microscopy and 100 exosomes per 10 µm polystyrene beads were used for capturing CD63 and CD9 positive exosomes.The polystyrene beads containing BSA instead of exosomes and with detector antibodies were used as a control.

somes were not shown in this paper due to the smaller size of exosomes, compared to ZIF-8 crystals. The fluorescent images showed the presence of CD81, CD9, CD63, EpCAM and PD-L1 positive exosomes captured on polystyrene beads (Fig. 3E). It is worth mentioning that the ZIF-8 platform showed auto-fluorescent characteristics, which was not beneficial in fluorescent imaging (data not shown).

3.3. Efficient immobilization of capture antibody on beads@ZIF-8/PDA-PEI

In order to achieve the optimized and highly sensitive conditions for exosome immune-capturing, three parameters should be considered carefully: (A) the total number of immune-captured beads acquired for the experiment, (B) the number of exosomes with a specific marker used for capture, and (C) optimal concentration of antibody required to get the best signal to noise ratio performance in a flow cytometer.

In this study, we used fluorescence labelled antibodies of the tetraspanin family (CD9, CD63, and CD81) as common exosome markers, as well as EpCAM (an epithelial marker enriched in carcinoma cells), and PD-L1 (Immune checkpoint inhibitor) [50] to evaluate and compare antibody immobilization efficiency between MOF coated beads and beads without MOF coating. To calculate the optimal concentration of anti-CD63, anti-CD81, anti-CD9, anti-EpCAM, and anti-PD-L1 capture antibodies sufficient for complete saturation of a 10 µm polystyrene bead, the following equation was implemented:

$$S = \frac{6}{\rho D} \times C \quad (1)$$

in which S is the required amount of protein for saturation of surface (mg protein/g of microspheres), C is the microsphere surface capacity for a given protein (mg protein/ m^2 of polymer surface), $6/\rho D$ is the surface area/mass (m^2/g) for microspheres of a known diameter (ρ is the density of microspheres, which for polystyrene is 1.05 g/cm^3), and D is the diameter of the microspheres, in micrometers. For IgG, C ~ 2.5 mg/m^2, and by comparing the MW of our ligand to that of IgG, surface saturation was approximated; 1.5 µg antibody needed for saturation of 1 mg 10 µm polystyrene beads, which in this experiment contains 1.87 × 10^6 beads.

The results indicated that the beads@ZIF-8/PDA-PEI showed higher MFI when 1.5 µg of anti-CD63-APC, anti-CD81-PE, anti-CD9-FITC, anti-EpCAM PE/Dazzle™ 594 and anti-PD-L1-PEcy7 antibodies per 1 mg beads were used. The detected MFI for 1.5 µg anti-CD63-APC, anti-CD81-PE, anti-CD9-FITC, anti-EpCAM-PE/Dazzle™ 594 and anti-PD-L1-PEcy7 antibodies immobilized on beads@ZIF-8/PDA-PEI platform was 15.2, 4.2, 2.1, 7.4 and 7.7 times higher respectively than the same amount of mentioned antibodies immobilized on polystyrene beads (Fig. 4A-E). Additionally, the detected MFI for 0.35 µg of anti-CD63-APC, anti-CD81-PE, anti-EpCAM-PE/Dazzle™ 594 and anti-PD-L1-PEcy7 antibodies immobilized on beads@ZIF-8/PDA-PEI platform was 6.8, 3.1, 3.5 and 3.5 times higher respectively than 1.5 µg of the anti-CD63-APC, anti-CD81-PE, anti-EpCAM-PE/Dazzle™ 594 and anti-PD-L1-PEcy7 immobilized on polystyrene beads (Fig. 4A-E).

To evaluate the efficiency of the MOF in the immobilization of antibodies and consequently the capturing of exosomes, a constant number of bead@ZIF-8/PDA-PEI,polystyrene beads, and EDC functionalized polystyrene beads was coated with a constant concentration of anti-CD81-PE, anti-CD9-FITC, anti-CD63-APC, anti-EpCAM-PE/Dazzle™ 594 and anti-PD-L1-PEcy7 antibodies and subjected to flow cytometry. As our polystyrene beads were rich in carboxyl functional groups on the surface, these groups could conjugate antibodies through passive adsorption. EDC was used for covalent functionalization of the capture antibodies to the carboxylate polystyrene beads through amide bond formation between the carboxyl groups on the surface of polystyrene beads and the primary amine groups of the protein. According to flow cytometry results for 1.5 µg anti-CD81-PE, anti-CD63-APC, anti-EpCAM- PE/Dazzle™ 594 and anti-PD-L1-PEcy7 immobilization on beads@ZIF-8/PDA-PEI platform, the detected MFI was 4.1, 8.1, 3.1 and 4.3 times higher respectively than the antibody immobilized on EDC-coated beads (Fig. 5A) which proves the better antibody immobilization on the surface. It is worth mentioning that the detected MFI for anti-CD9-FITC immobilized on the EDC-coated polystyrene beads versus beads@ZIF-8/PDA-PEI platform was similar.

Moreover, the measurement of the unbound antibody concentration presented in the supernatant showed that if 1.5 µg antibody per mg bead was used (in this experiment using 1.8 × 10^5 beads and 150 ng antibodies), more than 10–30 ng of the antibodies in the MOF platforms were redundant and were released in the supernatant (Fig. 5B). This means by decreasing the concentration of antibody in beads@ZIF-8/PDA-PEI platform, the specific antigen will be detected in flowcytometry. This proves that the platform not only provided the specific orientation for immobilized antibodies owing to the reduction of steric hindrance and tight confinement of the antibodies, but also inhibited the random and upside down orientation of the antibody, thus increasing the exposure of the antibody's antigen binding fragment to a higher amount of antigens. On the other hand, for both the polystyrene beads and beads functionalized with EDC, the concentration of the unbound antibodies were similar to each other and much lower than that of beads@ZIF-8/PDA-PEI. In this experiment, 100 ng of antibodies was sufficient to completely block the binding of 1.8 × 10^5 beads@ZIF-8/PDA-PEI which was much lower than polystyrene beads and beads coated with EDC.

3.4. Higher exosome capture efficiency in beads@ZIF-8/PDA-PEI compared to polystyrene beads

Here, we describe a facile and highly sensitive method for immunocapturing of exosomes followed by conventional flow cytometry detection to characterize small amounts of exosomes. According to Eq. (2) [21] the maximum number of exosomes captured per bead was calculated.

$$N = \frac{S_{bead}}{C_{exo}} \quad (2)$$

Where S_{bead} shows the surface of a sphere and C_{exo} shows the number of exosome circle surface that could fit in that area (the average diameter of exosome was considered 150 nm). A 10 µm polystyrene bead could attach to a maximum of 18,470 EVs. In our flow cytometry experiment, we used 50,000 beads for each run; a sample with 9.2 × 10^8 exosomes would saturate the beads. These calculations are based on the potential direct contact of the exosomes with the beads in the mix; because beads and exosomes have different physical behavior in solution owing to differences in their size and density, the beads would precipitate much faster than exosomes, which could remain in suspension longer. Therefore, the fluorescence intensity should be detected even if only half of the available surface of the bead was covered by exosomes, that is approximately 9000 exosomes. On the other hand, based on our previous results using ZIF-8/PDA-PEI platform which improved the LOD of ELISA by 225 times [47], the starting point for detecting the LOD of beads@ZIF-8/PDA-PEI for exosome markers was set at 1 × 10^7 followed by 5 × 10^6, 2.5 × 10^6 and 1.25 × 10^6 exosome particles (~ 250 ng, 125 ng, 62.5 ng and 31.2 ng of exosomes) enriched by ultracentrifugation from HeLa, MCF-7 and MDA-MB231 cell lines, which should provide a good signal for capture with 50,000 beads. A gating strategy was used to exclude bead aggregates and debris by forward scatter/side scatter (FSC/SSC) and

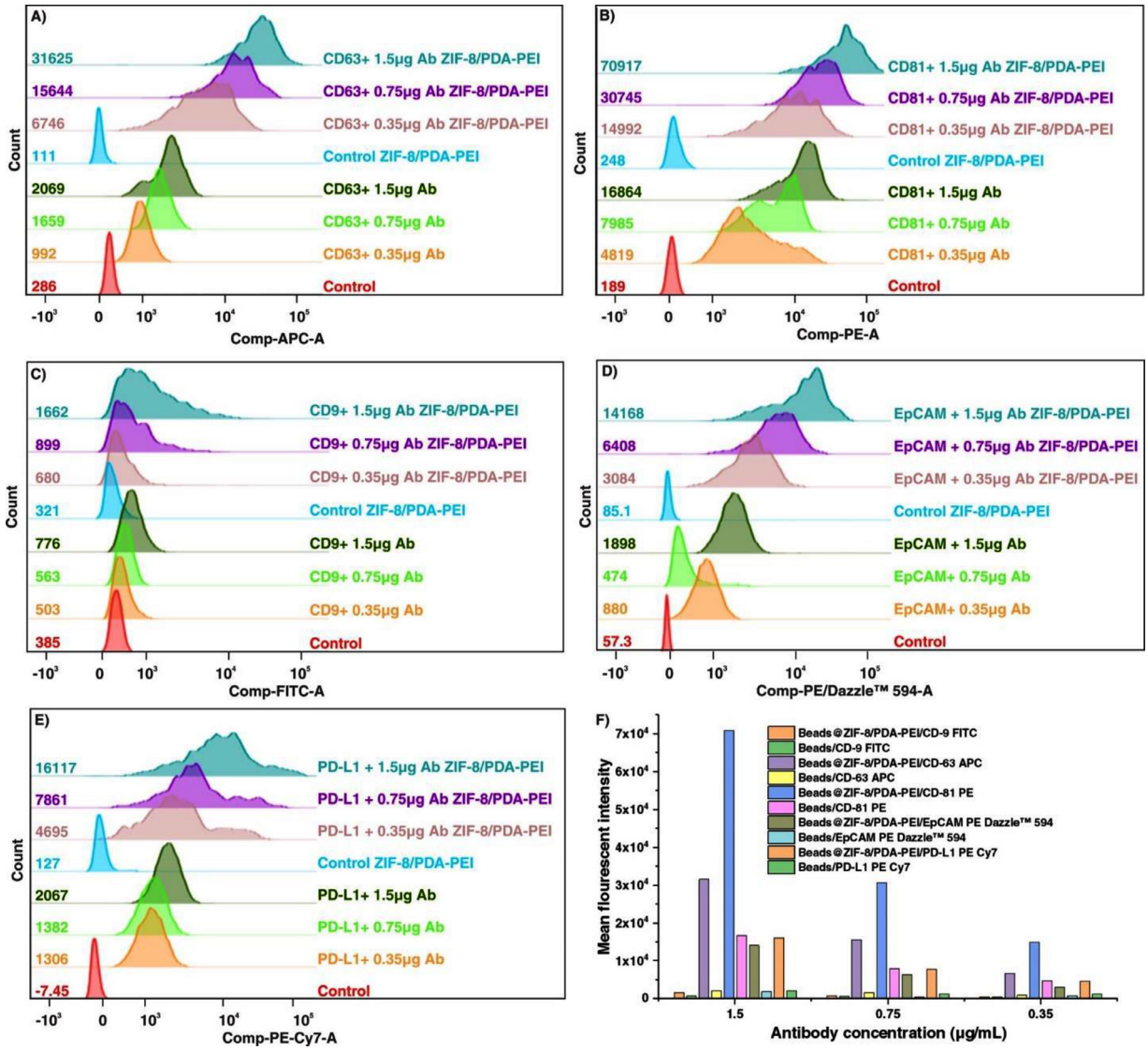

Fig. 4. Histogram overlay and detected MFI of capture antibody titration for evaluating the efficiency of ZIF-8/PDA-PEI on the immobilization of capture antibody on the surface of 10 µm polystyrene beads. (A) The concentrations of 1.5 µg, 0.75 µg and 0.35 µg of anti-CD63-APC antibody, (B) anti-CD81-PE antibody (C) anti-CD9-FITC antibody, (D) anti-EpCAM-PE/Dazzle™ 594 antibody and (E) anti-PD-L1-PE Cy7 antibody were immobilized on 1 mg of polystyrene beads and polystyrene beads@ZIF-8/PDA-PEI. (F) The chart of detected MFI for 1.5 µg, 0.75 µg and 0.35 µg of the anti-CD9-FITC, CD81-PE, CD63-APC, EpCAM-PE/Dazzle™ 594 and PD-L1- PE Cy7 antibodies immobilized on beads@ZIF-8/PDA-PEI platform versus polystyrene beads. In all experiments, the isotype control was used as a control and 50,000 beads were used for each run. (Ab stands for: antibody).

select the acquisition number in the region of PE, FITC, APC, PE Cy-7 and PE-Dazzle 594-positive microbeads. The strongest signal was detected when 200 exosomes per bead (1×10^7 particles, ~ 250 ng) was used in the beads@ZIF-8/PDA-PEI platform. The MFI detected for 200, 100, 50 and 25 PD-L1 positive exosomes of MDA-MB231 cell line per bead (corresponding to 250, 125, 62.5 and 31.2 ng) in beads@ZIF-8/PDA-PEI platform was 115, 348, 700 and 33 times higher than the MFI detected for the similar number of PD-L1 positive exosomes in non-coated polystyrene beads. Similarly, the MFI detected for 200 CD81, CD9 and CD63 positive exosomes per bead (~ 250 ng) in beads@ZIF-8/PDA-PEI platform was 2.1, 17 and 12.2 times higher than the MFI detected for the similar number of CD81, CD9 and CD63 positive exosomes in non-coated polystyrene beads. Additionally, the MFI detected for 200 EpCAM positive exosomes derived from MCF-7 cell line per bead (~ 250 ng) in beads@ZIF-8/PDA-PEI platform was 5.2 times higher than the MFI detected for the similar number of EpCAM positive exosomes in non-coated polystyrene beads (Fig. 6A-E). Results of exosome titration confirmed the high sensitivity of the assay with a positive signal detected when as little as 62.5 ng (2.5×10^6 particles) of exosomes were incubated with the beads, whereas ~5 µg (2×10^8 particles) was required for the detection of antibodies by Western Blotting.

The results indicated that coating the polystyrene beads with MOF increased the exosome capture efficiency 180 times compared to the conventional polystyrene bead immune affinity-based methods. In this way, we can detect as low as 50 exosomes per 10 µm polystyrene bead@ZIF-8/PDA-PEI, compared to 10 µm polystyrene beads that enable us to detect 9000 exosomes per bead. The minimum number of exosomes per bead that could be captured with bead@ZIF-8/PDA-PEI was 50 exosomes which could be attributed to the loss of large portion of exosomes in the polystyrene beads without MOF coating, so it has lower fluorescence signal. Results indicated that in our study the capture efficiency of MOF platform in three tetraspanins was not the same and CD63 showed higher expression (fluorescent intensity) in flow cytometry com-

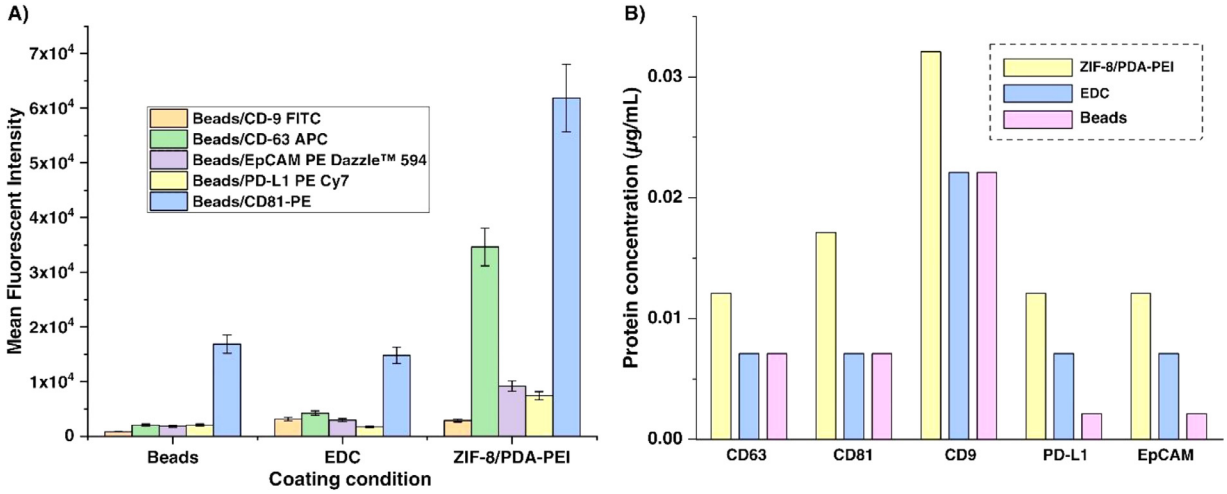

Fig. 5. The effect of ZIF-8/PDA-PEI coating on antibody immobilization. (A) The detected MFI of the immobilized anti-CD63-APC, anti-CD81-PE, anti-CD9-FITC, anti-EpCAM-PE/Dazzle^{TM} 594 and anti-PD-L1-PE Cy7 antibodies on the surface of 10 µm polystyrene beads versus carboxylate polystyrene beads functionalized with EDC and polystyrene beads@ZIF-8/PDA-PEI. (In all experiments, the isotype control was used as a control and 50,000 beads per test were used and 1.5 µg antibodies per 1 mg polystyrene beads were used for immobilization. (B) The comparison between the efficiency of antibody immobilization on carboxylate polystyrene beads versus polystyrene beads@ZIF-8/PDA-PEI and carboxylate polystyrene beads functionalized with EDC, was done by measuring the unbound antibody concentration presented in the supernatant. The anti-CD63, anti-CD81, anti-CD9, anti-EpCAM and anti-PD-L1, antibodies with the concentration of 150 ng, was co-incubated with 1.8×10^5 of 10 µm polystyrene beads.

pared to the CD9 and CD81 markers in exosmes derived from MDA-MB231, MCF-7 , and HeLa cell lines (Fig. 6F).

4. Discussion

Exosomes regarded as a promising component of the liquid biopsy methods, offering higher sensitivity and accuracy levels, and prompting continuing development of exosome capture and detection platforms. Recently, immunocapture methods for the characterization of exosome composition have gained increasing attention and several companies have commercialized kits to perform such assays [36]. The advantage of using antibodies for binding to a specific marker allows distinguishing between different exosome and other vesicle subpopulations generated from cells and facilitates the study of these diverse subpopulations selectively. However, currently there are no standardized immunocapture strategies and thus the sensitivities of these assays vary markedly. Studies have shown that the sensitivity for immunocapture aided flow cytometry (using microbeads) detection and characterization of exosomes relies on the relative size, number of microbeads and other related factors (e.g. surface area) of the exosomes in analysis [21,51]. Towards this, we proposed a novel nano-coating strategy based on MOFs to efficiently improve the LOD of current bead-based immunoaffinity assays for exosome detection using flow cytometry. This is the first time that a MOF coating has been used to improve the LOD for enhancing exosome captur efficiency through flow cytometry. This nano-coating strategy enabled us to detect as little as 50 exosomes per 10 µm polystyrene bead functionalized with ZIF-8/PDA-PEI, which is 180 times higher than the previously reported methods using naked microbeads [21,34]. The main factors that contributed to the improvement of the assay sensitivity, were increased surface area and hydrophilicity of the microbeads using the MOF platform. The platform also allowed the detection and characterization of exosome subpopulations by using both general exosome markers (tetraspanins) as well as EpCAM (marker for epithelial cancer cells) and PD-L1 (cancer biomarker). The results of this study are consistent with the study of Campos-Silva et al. [21], who could detect 30 ng of exosome in a streptavidin-biotin platform using 6 µm polystyrene beads. However, in this study we improved the LOD, while implementing the use of bigger polystyrene beads (10 µm size); also, in their platform 3200 EVs per bead were used for detection, while this platform enables us to detect as low as 50 exosomes per bead@ZIF-8/PDA-PEI. According to Eq. (2) and the flow cytometry data, we predict that by decreasing the diameter of the beads to 1 µm, we would be able to detect as low as five exosome per bead. However, this hypothesis needs to be confirmed by further experiments. The platform enabled us to develop a ready to use and cost-effective platform to measure the expression of low-expressed antigens in exosomes with much higher sensitivity.

The results of this study showed similar sensitivity compared to the results of Sun et al., who used Zr-MOFs encapsulated with methylene blue to detect the concentration of exosomes by monitoring the electroactive molecules inside [52]. Their platform could be used to detect exosomes ranging from 9.5×10^3 to 1.9×10^7 particles/µL with a detection limit of 7.83×10^3 particles/µL, which is comparable to our platform. Several other methods, such as alternating current electrohydrodynamic induced nanoshearing [53], an integrated magneto-electrochemical sensor [54], aptasensor DNA-capped single-walled carbon nanotubes [55], Zirconium-mediated signal amplification [52] and Copper-mediated exosome detection have been developed to improve the LOD of exosomes [56]. Comparatively, in our study the beads@ZIF-8/PDA-PEI had a higher sensitivity and facile performance [57].

Exosome detection techniques have also been explored with the aid of microfluidic technology. Towards this, Zhang et al. [58], introduced an ExoProfile chip that was constructed of 3D porous serpentine nanostructures to provide enormous reaction sites and improved biosensing efficiency of exosomes. The device was validated with purified exosomes from SKOV3 cells, which yielded a LOD of 21 exosomes per mL within 3 h. Bai et al. used a bead-based microarray platform using quantum dot probes, to facilitate multiplexed detection of exosome (derived from lung cancer cells) surface protein markers [37]. Fang et al. also developed a microfluidic device to perform on-chip exosome immunocapture and specific marker detection from both cell culture medium and plasma of human breast cancer-derived samples [36]. Despite the ongoing development of microfluidic technology [59], the statistical limitation of small sample sizes using this technology, limits the potential for these techniques to be scaled up for clinical and diagnostic applications [60]. Several attempts have been made to improve the LOD and the sensitivity of exosome detection methods, as summarized

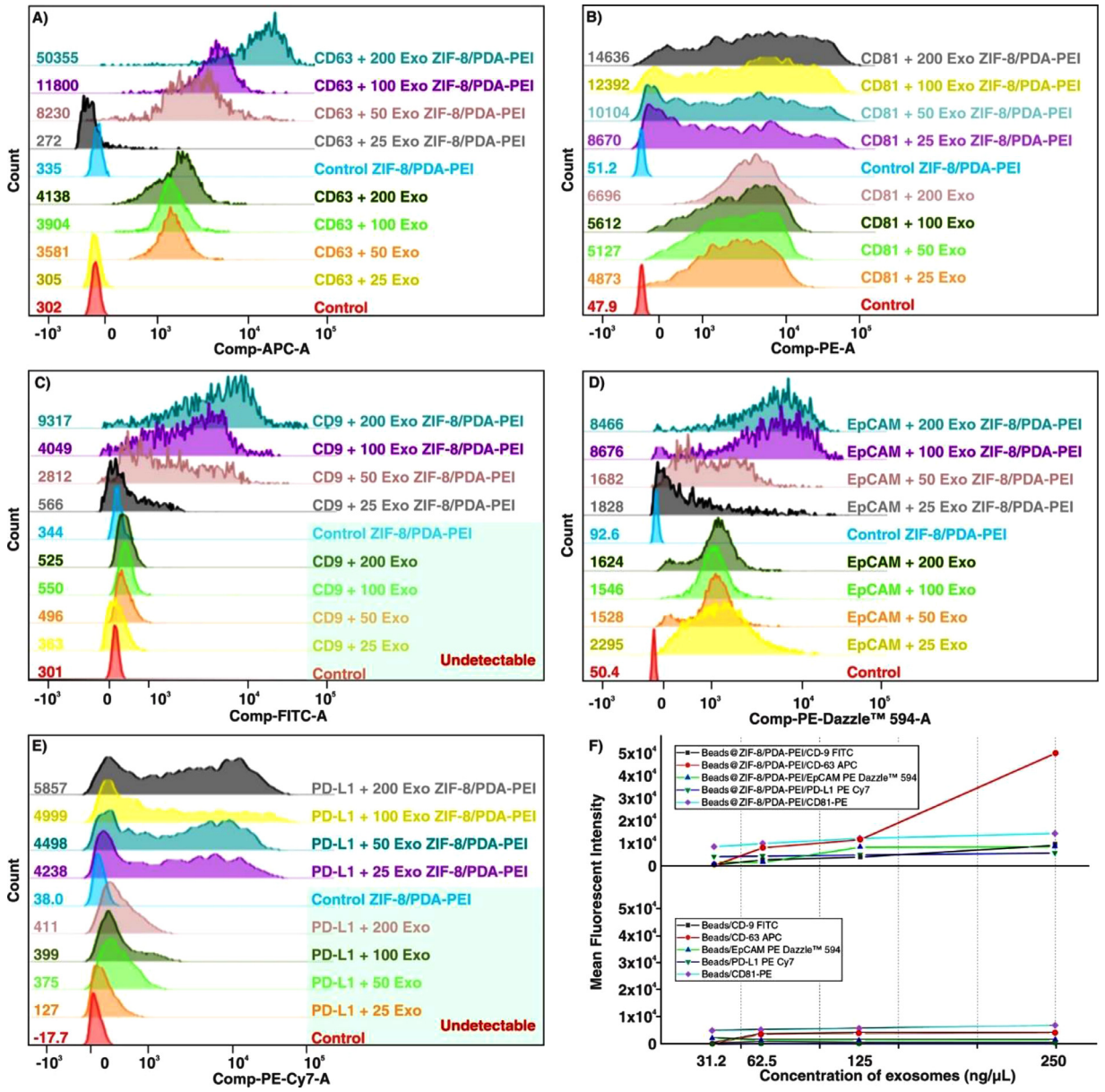

Fig. 6. Histogram overlay of exosome titration for evaluating the efficiency of ZIF-8/PDA-PEI on the detection of exosomes using flow cytometry. (A) Histogram overlay and MFI detected in exosome titration process, using 200, 100, 50 and 25 exosomes per polystyrene bead labeled with 1.5 μg of anti-CD63 capture and anti-CD63-APC detector antibody, (B) anti-CD81 capture and anti-CD81-PE detector antibody, (C) anti-CD9 capture and anti-CD9-FITC detector antibody, (D) anti-EpCAM capture and anti-EpCAM-PE/Dazzle™ 594 detector antibody and (E) anti-PD-L1 capture and anti-PD-L1-PE Cy7 detector antibody per 1 mg of polystyrene beads versus polystyrene beads@ZIF-8/PDA-PEI. In all experiments, the isotype control was used as a control and 50,000 beads per test were used. (F) The chart of LOD detected for 200,100, 50 and 25 CD63, CD81, CD9, EpCAM and PD-L1 positive exosomes (~ 250 ng, 125 ng, 62.5 ng and 31.2 ng) captured on the surface of each beads@ZIF-8/PDA-PEI platform versus polystyrene beads. For detecting EpCAM and PD-L1 positive exosomes, the MCF-7 and MDA-MB231 cell lines were used, respectively. In all experiments, beads coated with BSA was used as a control and 50,000 beads per test were used. (Exo stands for: Exosome).

by Wang et al. [57] and there are numerous commercial immunoaffinity beads for exosome detection, which we name here few of them. The CD63 Exosome Capture Beads (ab239686) could detect 2.4 × 10^9 exosomes, while using our platform, we are able to detect 1.25 × 10^6 particles. Another example is the Exosome – Human CD63 Isolation/Detection Invitrogen (10606D), which could detect 25 μg of total protein.

In this study, we have introduced a facile, reproducible, highly sensitive, and affordable method for the detection of exosomes by using MOFs to achieve a higher antibody immobilization density. The results indicated that coating beads with MOF increased the capture efficiency since the coated MOFs have large surface area (typically ranging from 1000 to 10,000 m^2/g) that increases interactions between the substrates and analytes, leads to higher absorption and sensitivity of detection. Furthermore, in this platform, a higher antibody immobilization density could be achieved to promote greater physical adsorption of the antibody onto the polystyrene surface owing to an increase in the surface roughness and providing a larger surface area.. More importantly, due to the characteristics of ZIF-8 MOFs, the exosomes could easily be detached from the beads (within 30 min in EDTA (pH 5.0)) without the use of harmful chemicals [40]. These advantages cumulatively make the MOFs an ideal candidate to achieve high fluorescent intensity in the detection of exosome markers by flow cytometry, while consuming a much lower concentration of antibodies.

5. Conclusions

In this study, we demonstrated a new approach for exosome immunocapture and flow cytometry analysis using ZIF-8 as representative of MOF in the beads@ZIF-8/PDA-PEI platform that provides much higher sensitivity and capture efficiency than commercial microbeads. The proposed platform also improved the LOD for CD63, CD81, CD9, EpCAM, and PD-L1 exosome and cancer markers by 180 times compared to conventional detection of exosome based on microbeads and allowed the detection of 50 exosome particles per bead. The implication of flow cytometry using MOF functionalized beads for the study of multiple exosome markers using combinations of several fluorescent antibodies provided the advantage of facilitating highly sensitive detection and characterization of exosome markers. This platform can perform highly efficient detection of exosomes in most laboratories with access to conventional flow cytometry. The bead@ZIF-8/PDA-PEI platform can be used to sort subpopulations of exosomes from the heterogeneous bulk samples effectively, using a FACS cell sorter machine. Additionally, the proposed platform enabled us to release exosomes from the bead@ZIF-8/PDA-PEI platform without the use of harmful chemicals that could potentially destroy the exosomes. The MOF platform enjoys several advantages over most current exosome detection and characterization techniques, most notably achieving significantly enhanced LOD from samples containing low exosome amounts. Based on the results of this study, future experiments of the group will further explore exosome detection from samples containing even fewer exosome amounts.

Author contributions

Conceptualization: Majid Ebrahimi Warkiani.; writing—original draft preparation: Sareh Zhand. ; writing—review and editing: Sareh Zhand, Sajad Razavi Bazaz, Ying Zhu, Majid Ebrahimi Warkiani.; supervision: Dayong Jin, Majid Ebrahimi Warkiani.; manuscript revision: Sareh Zhand, Sajad Razavi Bazaz,Ying Zhu, Majid Ebrahimi Warkiani.

Declaration of Competing Interest

The authors declare that they have no known competing financial interests or personal relationships that could have appeared to influence the work reported in this paper.

Acknowledgment

The authors would like to warmly thank the Australian Research Council for the support of this project through Discovery Project Grants (DP170103704 and DP180103003) as well as the National Health and Medical Research Council for the Career Development Fellowship (APP1143377). We would also like to thank South Australian node of the Australian National Fabrication Facility under the National Collaborative Research Infrastructure Strategy.

References

[1] M. He, J. Crow, M. Roth, Y. Zeng, A.K. Godwin, Integrated immunoisolation and protein analysis of circulating exosomes using microfluidic technology, Lab Chip 14 (19) (2014) 3773–3780.
[2] J.D. Schiffman, P.G. Fisher, P. Gibbs, Early detection of cancer: past, present, and future, Am. Soc. Clin. Oncol. Educ. Book 35 (1) (2015) 57–65.
[3] F.S. Iliescu, D.P. Poenar, F. Yu, M. Ni, K.H. Chan, I. Cima, et al., Recent advances in microfluidic methods in cancer liquid biopsy, Biomicrofluidics 13 (4) (2019) 041503.
[4] S.A. Melo, L.B. Luecke, C. Kahlert, A.F. Fernandez, S.T. Gammon, J. Kaye, et al., Glypican-1 identifies cancer exosomes and detects early pancreatic cancer, Nature 523 (7559) (2015) 177–182.
[5] J. Eyles, A.-L. Puaux, X. Wang, B. Toh, C. Prakash, M. Hong, et al., Tumor cells disseminate early, but immunosurveillance limits metastatic outgrowth, in a mouse model of melanoma, J. Clin. Invest. 120 (6) (2010) 2030–2039.
[6] T.M. Gall, S. Belete, E. Khanderia, A.E. Frampton, L.R. Jiao, Circulating tumor cells and cell-free DNA in pancreatic ductal adenocarcinoma, Am. J. Pathol. 189 (1) (2019) 71–81.
[7] M. Nawaz, G. Camussi, H. Valadi, I. Nazarenko, K. Ekström, X. Wang, et al., The emerging role of extracellular vesicles as biomarkers for urogenital cancers, Nat. Rev. Urol. 11 (12) (2014) 688.
[8] G. Szabo, F. Momen-Heravi, Extracellular vesicles in liver disease and potential as biomarkers and therapeutic targets, Nat. Rev. Gastroenterol. Hepatol. 14 (8) (2017) 455.
[9] S.-J. Dawson, D.W. Tsui, M. Murtaza, H. Biggs, O.M. Rueda, S.-F. Chin, et al., Analysis of circulating tumor DNA to monitor metastatic breast cancer, N. Engl. J. Med. 368 (13) (2013) 1199–1209.
[10] W. Wang, J. Luo, S. Wang, Recent progress in isolation and detection of extracellular vesicles for cancer diagnostics, Adv. Healthc. Mater. 7 (20) (2018) 1800484.
[11] C. Théry, L. Zitvogel, S. Amigorena, Exosomes: composition, biogenesis and function, Nat. Rev. Immunol. 2 (8) (2002) 569–579.
[12] R. Cazzoli, F. Buttitta, M. Di Nicola, S. Malatesta, A. Marchetti, W.N. Rom, et al., microRNAs derived from circulating exosomes as noninvasive biomarkers for screening and diagnosing lung cancer, J. Thoracic Oncol. 8 (9) (2013) 1156–1162.
[13] J. Skog, T. Würdinger, S. Van Rijn, D.H. Meijer, L. Gainche, W.T. Curry, et al., Glioblastoma microvesicles transport RNA and proteins that promote tumour growth and provide diagnostic biomarkers, Nat. Cell Biol. 10 (12) (2008) 1470–1476.
[14] S. Kourembanas, Exosomes: vehicles of intercellular signaling, biomarkers, and vectors of cell therapy, Annu. Rev. Physiol. 77 (2015) 13–27.
[15] A.J. Szempruch, S.E. Sykes, R. Kieft, L. Dennison, A.C. Becker, A. Gartrell, et al., Extracellular vesicles from Trypanosoma brucei mediate virulence factor transfer and cause host anemia, Cell 164 (1–2) (2016) 246–257.
[16] L. Gangoda, S. Boukouris, M. Liem, H. Kalra, S. Mathivanan, Extracellular vesicles including exosomes are mediators of signal transduction: are they protective or pathogenic? Proteomics 15 (2–3) (2015) 260–271.
[17] A. Hoshino, B. Costa-Silva, T.-L. Shen, G. Rodrigues, A. Hashimoto, M.T. Mark, et al., Tumour exosome integrins determine organotropic metastasis, Nature 527 (7578) (2015) 329–335.
[18] L. Zhang, S. Zhang, J. Yao, F.J. Lowery, Q. Zhang, W.-C. Huang, et al., Microenvironment-induced PTEN loss by exosomal microRNA primes brain metastasis outgrowth, Nature 527 (7576) (2015) 100–104.
[19] G. Van Niel, I. Porto-Carreiro, S. Simoes, G. Raposo, Exosomes: a common pathway for a specialized function, J. Biochem. 140 (1) (2006) 13–21.
[20] X.-X. Yang, C. Sun, L. Wang, X.-L. Guo, New insight into isolation, identification techniques and medical applications of exosomes, J. Controll. Release (2019).
[21] C. Campos-Silva, H. Suárez, R. Jara-Acevedo, E. Linares-Espinós, L. Martinez-Piñeiro, M. Yáñez-Mó, et al., High sensitivity detection of extracellular vesicles immune-captured from urine by conventional flow cytometry, Sci. Rep. 9 (1) (2019) 1–12.
[22] S. Lin, Z. Yu, D. Chen, Z. Wang, J. Miao, Q. Li, et al., Progress in microfluidics-based exosome separation and detection technologies for diagnostic applications, Small 16 (9) (2020) 1903916.
[23] A. Gámez-Valero, M. Monguió-Tortajada, L. Carreras-Planella, K. Beyer, F.E. Borràs, Size-exclusion chromatography-based isolation minimally alters extracellular vesicles' characteristics compared to precipitating agents, Sci Rep. 6 (2016) 33641.
[24] A. Böing, E. Van Der Pol, A. Grootemaat, Single-step isolation of extracellular vesicles from plasma by size-exclusion chromatography, J. Extracell. Vesicles 3 (2014) 118.
[25] A. de Menezes-Neto, M.J.F. Sáez, I. Lozano-Ramos, J. Segui-Barber, L. Martin-Jaular, J.M.E. Ullate, et al., Size-exclusion chromatography as a stand-alone methodology identifies novel markers in mass spectrometry analyses of plasma-derived vesicles from healthy individuals, J. Extracell. Vesicles 4 (1) (2015) 27378.
[26] Livshits M.A., Khomyakova E., Evtushenko E.G., Lazarev V.N., Kulemin N.A., Semina S.E., et al. Isolation of exosomes by differential centrifugation: theoretical analysis of a commonly used protocol. 2015;5:17319.
[27] M.Y. Konoshenko, E.A. Lekchnov, A.V. Vlassov, P.P. Laktionov, Isolation of extracellular vesicles: general methodologies and latest trends, Biomed. Res. Int. (2018) 2018.
[28] Sidhom K., Obi P.O., Saleem AJljoms. A review of exosomal isolation methods: is size exclusion chromatography the best option? 2020;21(18):6466.
[29] A.F. Orozco, D.E. Lewis, Flow cytometric analysis of circulating microparticles in plasma, Cytometry Part A 77 (6) (2010) 502–514.
[30] E. Van Der Pol, A. Hoekstra, A. Sturk, C. Otto, T. Van Leeuwen, R. Nieuwland, Optical and non-optical methods for detection and characterization of microparticles and exosomes, J. Thrombosis Haemostasis 8 (12) (2010) 2596–2607.
[31] J. Lötvall, A.F. Hill, F. Hochberg, E.I. Buzás, D. Di Vizio, C. Gardiner, et al., Minimal Experimental Requirements for Definition of Extracellular Vesicles and Their functions: a Position Statement from the International Society for Extracellular Vesicles, Taylor & Francis, 2014.
[32] C. Gorgun, D. Reverberi, G. Rotta, F. Villa, R. Quarto, R. Tasso, Isolation and flow cytometry characterization of extracellular-vesicle subpopulations derived from human mesenchymal stromal cells, Curr. Protoc. Stem. Cell Biol. 48 (1) (2019) e76.
[33] P. Sharma, S. Ludwig, L. Muller, C.S. Hong, J.M. Kirkwood, S. Ferrone, et al., Immunoaffinity-based isolation of melanoma cell-derived exosomes

from plasma of patients with melanoma, J. Extracell. Vesicles 7 (1) (2018) 1435138.
[34] W. Nakai, T. Yoshida, D. Diez, Y. Miyatake, T. Nishibu, N. Imawaka, et al., A novel affinity-based method for the isolation of highly purified extracellular vesicles, Sci. Rep. 6 (2016) 33935.
[35] Chen C., Skog J., Hsu C.-.H., Lessard R.T., Balaj L., Wurdinger T., et al. Microfluidic isolation and transcriptome analysis of serum microvesicles. 2010;10(4):505–11.
[36] S. Fang, H. Tian, X. Li, D. Jin, X. Li, J. Kong, et al., Clinical application of a microfluidic chip for immunocapture and quantification of circulating exosomes to assist breast cancer diagnosis and molecular classification, PLoS ONE 12 (4) (2017) e0175050.
[37] Y. Bai, Y. Lu, K. Wang, Z. Cheng, Y. Qu, S. Qiu, et al., Rapid isolation and multiplexed detection of exosome tumor markers via queued beads combined with quantum dots in a microarray, Nano-Micro Lett. 11 (1) (2019) 59.
[38] J.A. Welsh, J.A. Holloway, J.S. Wilkinson, N.A. Englyst, Extracellular vesicle flow cytometry analysis and standardization, Front. Cell Dev. Biol. 5 (2017) 78.
[39] S. Afreen, Z. He, Y. Xiao, J.-.J. Zhu, Nanoscale metal–organic frameworks in detecting cancer biomarkers, J. Mater. Chem. B (2020).
[40] Feng Y., Wang H., Zhang S., Zhao Y., Gao J., Zheng Y., et al. Antibodies@ MOFs: an in vitro protective coating for preparation and storage of biopharmaceuticals. 2019;31(2):1805148.
[41] A. Razmjou, M. Asadnia, O. Ghaebi, H.-.C. Yang, M. Ebrahimi Warkiani, J. Hou, et al., Preparation of Iridescent 2D photonic crystals by using a mussel-inspired spatial patterning of ZIF-8 with potential applications in optical switch and chemical sensor, ACS Appl. Mater. Interfaces 9 (43) (2017) 38076–38080.
[42] Liang K., Ricco R., Doherty C.M., Styles M.J., Bell S., Kirby N., et al. Biomimetic mineralization of metal-organic frameworks as protective coatings for biomacromolecules. 2015;6:7240.
[43] Huang G., Lin G., Zhu Y., Duan W., Jin DJLoaC. Emerging technologies for profiling extracellular vesicle heterogeneity. 2020;20(14):2423–37.
[44] M. Mohammad, A. Razmjou, K. Liang, M. Asadnia, V. Chen, Metal–Organic-Framework-Based Enzymatic Microfluidic Biosensor via Surface Patterning and Biomineralization, ACS Appl. Mater. Interfaces 11 (2) (2018) 1807–1820.
[45] H. Lee, S.M. Dellatore, W.M. Miller, P.B. Messersmith, Mussel-inspired surface chemistry for multifunctional coatings, Science 318 (5849) (2007) 426–430.
[46] Y. Tian, Y. Cao, Y. Wang, W. Yang, J. Feng, Realizing ultrahigh modulus and high strength of macroscopic graphene oxide papers through crosslinking of mussel-inspired polymers, Adv. Mater. 25 (21) (2013) 2980–2983.
[47] Zhand S., Razmjou A., Azadi S., Razavi Bazaz S., Shrestha J., Asadnia Fard Jahromi M., et al. A Metal–Organic Framework-Enhanced ELISA Platform for Ultrasensitive Detection of PD-L1. 2020.
[48] J. Beauchamp, Infrared Tables (short summary of common absorption frequencies), Course Notes 2620 (2010) 19.
[49] W. Wong-Ng, J. Kaduk, L. Espinal, M. Suchomel, A. Allen, H. Wu, High-resolution synchrotron X-ray powder diffraction study of bis (2-methylimidazolyl)-zinc, C 8 H 10N 4Zn (ZIF-8), Powder Diffr. 26 (3) (2011) 234–237.
[50] S. Azadi, H. Aboulkheyr Es, S. Razavi Bazaz, J.P. Thiery, M. Asadnia, M Ebrahimi Warkiani, Upregulation of PD-L1 expression in breast cancer cells through the formation of 3D multicellular cancer aggregates under different chemical and mechanical conditions, Biochimica et Biophysica Acta (BBA) - Mol. Cell Res. 1866 (12) (2019) 118526.
[51] S. Mastoridis, G.M. Bertolino, G. Whitehouse, F. Dazzi, A. Sanchez-Fueyo, M. Martinez-Llordella, Multiparametric analysis of circulating exosomes and other small extracellular vesicles by advanced imaging flow cytometry, Front. Immunol. 9 (1583) (2018).
[52] Z. Sun, L. Wang, S. Wu, Y. Pan, Y. Dong, S. Zhu, et al., An electrochemical biosensor designed by using Zr-based metal–organic frameworks for the detection of glioblastoma-derived exosomes with practical application, Anal. Chem. 92 (5) (2020) 3819–3826.
[53] R. Vaidyanathan, M. Naghibosadat, S. Rauf, D. Korbie, L.G. Carrascosa, M.J. Shiddiky, et al., Detecting exosomes specifically: a multiplexed device based on alternating current electrohydrodynamic induced nanoshearing, Anal. Chem. 86 (22) (2014) 11125–11132.
[54] S. Jeong, J. Park, D. Pathania, C.M. Castro, R. Weissleder, H. Lee, Integrated magneto–electrochemical sensor for exosome analysis, ACS Nano 10 (2) (2016) 1802–1809.
[55] Y. Xia, M. Liu, L. Wang, A. Yan, W. He, M. Chen, et al., A visible and colorimetric aptasensor based on DNA-capped single-walled carbon nanotubes for detection of exosomes, Biosens. Bioelectron. 92 (2017) 8–15.
[56] F. He, J. Wang, B.-.C. Yin, B.-.C. Ye, Quantification of exosome based on a copper-mediated signal amplification strategy, Anal. Chem. 90 (13) (2018) 8072–8079.
[57] Q. Wang, L. Zou, X. Yang, X. Liu, W. Nie, Y. Zheng, et al., Direct quantification of cancerous exosomes via surface plasmon resonance with dual gold nanoparticle-assisted signal amplification, Biosens. Bioelectron. 135 (2019) 129–136.
[58] P. Zhang, X. Zhou, Y. Zeng, Multiplexed immunophenotyping of circulating exosomes on nano-engineered ExoProfile chip towards early diagnosis of cancer, Chem. Sci. 10 (21) (2019) 5495–5504.
[59] S. Razavi Bazaz, H.A. Amiri, S. Vasilescu, A. Abouei Mehrizi, D. Jin, M. Miansari, et al., Obstacle-free planar hybrid micromixer with low pressure drop, Microfluid Nanofluidics 24 (8) (2020) 61.
[60] A.S. Rzhevskiy, S. Razavi Bazaz, L. Ding, A. Kapitannikova, N. Sayyadi, D. Campbell, et al., Rapid and label-free isolation of tumour cells from the urine of patients with localised prostate cancer using inertial microfluidics, Cancers (Basel) 12 (1) (2019) 81.